p27 is involved in N-cadherin-mediated contact inhibition of cell growth and S-phase entry

Shulamit Levenberg, Anat Yarden, Zvi Kam and Benjamin Geiger

Department of Molecular Cell Biology, The Weizmann Institute of Science, Rehovot 76100, Israel

In this study the direct involvement of cadherins in adhesion-mediated growth inhibition was investigated. It is shown here that overexpression of N-cadherin in CHO cells significantly suppresses their growth rate. Interaction of these cells and two additional fibroblastic lines with synthetic beads coated with N-cadherin ligands (recombinant N-cadherin ectodomain or specific antibodies) leads to growth arrest at the G1 phase of the cell cycle. The cadherin-reactive beads inhibit the entry into S phase and the reduction in the levels of cyclin-dependent kinase (cdk) inhibitors p21 and p27, following serum-stimulation of starved cells. In exponentially growing cells these beads induce G1 arrest accompanied by elevation in p27 only. We propose that cadherin-mediated signaling is involved in contact inhibition of growth by inducing cell cycle arrest at the G1 phase and elevation of p27 levels.

Keywords: cell adhesion; cadherin; cell growth; cell cycle; p27

Introduction

The rate of proliferation of most non-transformed adherent cells decreases as their density on the substratum increases, a phenomenon commonly known as density-dependent-inhibition, or contact-inhibition of growth (Deleu *et al.*, 1998; Dietrich *et al.*, 1997; Kato *et al.*, 1997; Polyak *et al.*, 1994a; Weiser *et al.*, 1985; Holley, 1975). The loss of this contact responsiveness can lead to deregulated growth and formation of multi-layered foci in culture, a phenomenon which is commonly associated with malignant transformation (Becker *et al.*, 1994; Tsukita *et al.*, 1993). The molecular mechanisms responsible for growth inhibition in dense cultures are poorly understood, and in particular it is not clear whether it involves signaling processes triggered by specific adhesion molecules (Kato *et al.*, 1997; Weiser and Oesch, 1986). It was however established that contact-inhibited cells are arrested at the G1 phase of the cell cycle (Deleu *et al.*, 1998; Dietrich *et al.*, 1997; Polyak *et al.*, 1994a). Recent studies indicated that upon reaching confluence, cellular levels of the cdk inhibitor p27 increase (Polyak *et al.*, 1994a) and the activity of cdk4 decreases (Deleu *et al.*, 1998). Recently it has been shown that the modulation of cadherin-mediated interactions by low Ca^{2+} medium or by inhibitory

antibodies can stimulate cell proliferation (Kandikonda *et al.*, 1996) while overexpression of VE-cadherin can inhibit cell growth (Caveda *et al.*, 1996). Moreover, coating of the underlying substratum with the extracellular domain of recombinant VE-cadherin apparently suppresses cell prolifertion (Caveda *et al.*, 1996).

In this study we have tested the hypothesis that surface clustering of the adherens junction molecule N-cadherin can generate growth inhibitory signals. We show here that chinese hamster ovary (CHO) cells expressing different levels of N-cadherin display reduced growth rates, and that normal growth can be restored by cadherin inhibitory antibodies. We further show that synthetic beads coated with N-cadherin ligands including N-cadherin extracellular domain (NEC) and cadherin-specific antibodies (Levenberg *et al.*, 1998a) can block S-phase entry in N-cadherin transfected CHO cells as well as additional fibroblastic lines. Moreover these beads, when applied to exponentially growing cells induce an increase in the levels of the cdk inhibitor p27 and arrest cell growth at G1.

Results

Specific suppression of growth by transfection of CHO cells with N-cadherin cDNA

Stably transfected CHO cells expressing different levels of N-cadherin were shown to grow at a significantly slower rate (60–65%) compared to the parental CHO cells (Figure 1a). The expression of N-cadherin in CHO cells (FL4 cell line) was also accompanied by a reduction in the number of cells in S phase of the cell cycle following 2–3 days in culture. Thus, the percentage of FL4 cells in S phase following 2 or 3 days in culture was 34% or 15% respectively, compared to 50% or 35% in nontransfected CHO cells, cultured under the same conditions (Figure 1b). This growth inhibition can be primarily attributed to the presence of N-cadherin, since inhibitory antibodies directed against the extracellular domain of this molecule completely abolish it (Figure 1c).

The effect of cadherin-reactive beads on S-phase entry after serum stimulation of starved cells

To test the direct involvement of N-cadherin in growth regulation we have added to sparsely plated cells 6 μm beads covalently coupled to recombinant N-cadherin ectodomain (NEC) or to purified anti N-cadherin antibodies (BE) (Volk and Geiger, 1986). We have previously shown that when such beads bind to N-cadherin-transfected CHO cells, the junctional labeling
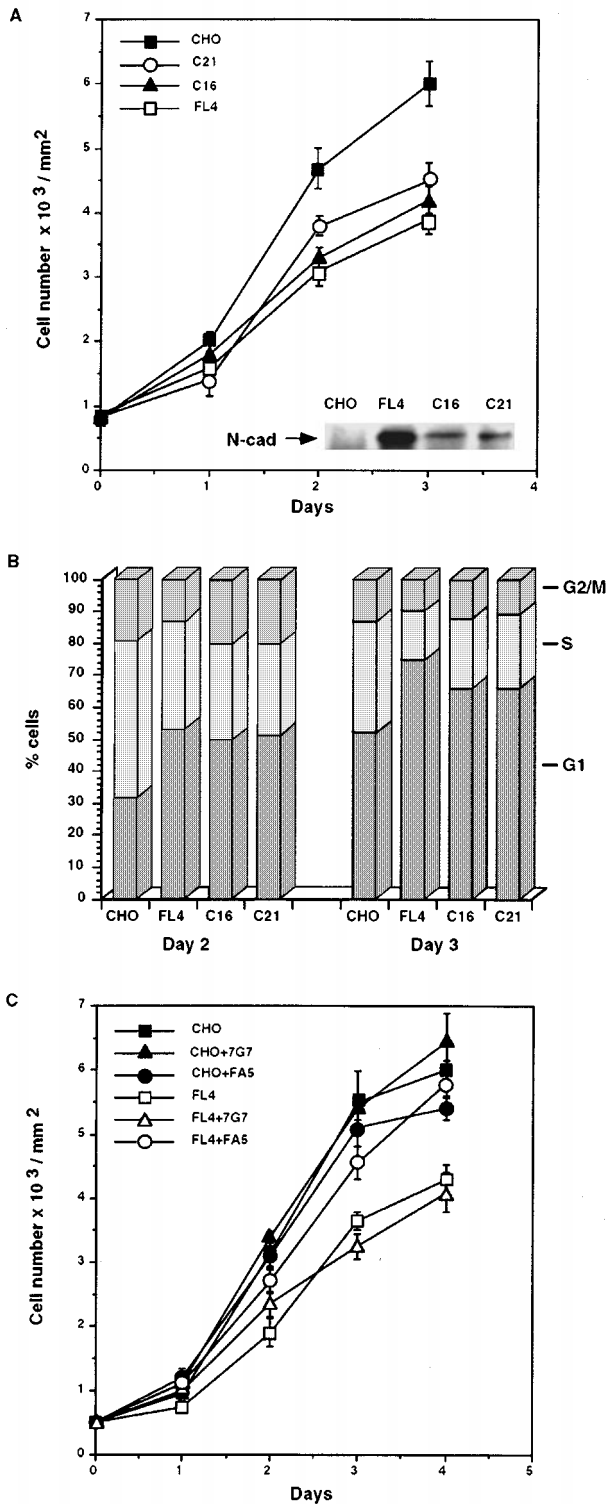
Figure 1 Effect of N-cadherin expression on the growth rate of transfected CHO cells. (**a**) Growth curves of CHO-derived cell lines expressing different levels of N-cadherin. Parental CHO cells as well as stable clones of CHO cells, which express chicken N-cadherin (FL4, C16 and C21, relative cadherin levels are shown by Western blot analysis in the insert) were plated at about 20% confluence and the numbers of viable cells were counted in tetraplicates over the subsequent 3 days. (**b**) Cell cycle distribution of CHO cells expressing different levels of N-cadherin. Flow cytometric analysis of Propidium Iodide-stained subconfluent monolayers of CHO cells (as in **a**) at the second (day 2) and third day (day 3) after plating. (**c**) Growth curves of N-cadherin-transfected CHO cells (clone FL4) and parental CHO cells in the presence of N-cadherin-specific (FA5) and control irrelevant (7G7) antibodies. Note that the growth rate of FL4 cells in the presence of the inhibitory FA5 antibodies was similar to that of the parental CHO cells

for N-cadherin, β-catenin, vinculin and phosphotyrosine increases (Levenberg *et al.*, 1998a). Here we have employed a similar approach to determine the effect of immobilized cadherin-specific ligands (NEC and BE) on the growth of cells expressing the appropriate cadherin by examining their cell cycle profile. To specifically study the cell cycle in those cells which interact with the cadherin reactive (or control) beads we have developed a quantitative microscopic system for cell cycle analysis based on DNA content (determined by DAPI staining) and BrdU incorporation in cells which are in direct contact with beads. Plotting BrdU immunofluorescence intensity against the fluorescent intensity of DAPI enables a distinction between cells at G1, S and G2/M phases of the cell cycle (see for example the right column in Figure 5).

To study the effect of cadherin reactive beads on G1- to S-transition, we have serum-starved FL4 cells for 72 h, then added the various beads together with serum-containing medium. At different time points thereafter cells were pulsed with BrdU for 30 min, fixed and fluorescently labeled for BrdU and DNA content (DAPI). Representative images of superpositions of the BrdU (red) and DAPI (blue) labeling, as well as the positions of the various beads are shown in Figure 2. Note that pink-colored nuclei are those that were in S-phase during the BrdU pulse. The effect of the various beads on the emergence of FL4, Swiss-3T3 and Rat-1 cells into S-phase after serum stimulation is shown in Figure 3. For FL4 cells, the incubation with beads coated with either NEC or BE antibodies significantly reduced the initial emergence of cells into S-phase, and most effectively suppressed cell entry to S-phase following additional incubation for 1–2 days. ConA-coated beads did not have such effect, and fibronectin-coated beads were even slightly stimulatory. Strong suppression of S-phase entry by NEC-coated beads was also obtained with the other fibroblastic lines (Swiss-3T3 and Rat-1) which express an endogenous N-cadherin. The effect was particularly dramatic in Swiss-3T3 cells, in which no increase in S-phase cells was noticed in the cells associated with the cadherin-conjugated beads after serum stimulation.

The possible mechanism underlying the effect of cadherin-reactive beads on the cell-cycle machinery was studied by immunoblot analysis of the retinoblastoma protein (pRb) and the cdk inhibitors, p21 and p27 in beads-attached Swiss-3T3 cells. As shown in Figure 4, most of the pRb in serum-starved cells (about 75%) is in the hypophosphorylated state (lower band in Figure 4a), while within 48 h after the addition of serum-containing medium, the levels of phosphorylated and hypophosphorylated pRb become roughly equal. ConA-coupled beads had no effect on pRb phosphorylation state, while NEC-coated beads induced an increase in the relative levels of the hypophosphorylated molecule to approximately 65%. There were no significant changes in the overall levels of pRb in the various bead-treated samples. Taking into account the fact that only part of the cells (roughly 50–70%) physically interact with the beads, the actual cadherin-mediated suppression of pRb phosphorylation in the cells which are in direct contact with beads is even higher. Serum starvation of Swiss-3T3 cells induced marked increases in the levels of the two cdk inhibitors p21 and p27 (Figure 4b and c, see Coats *et al.*, 1996;
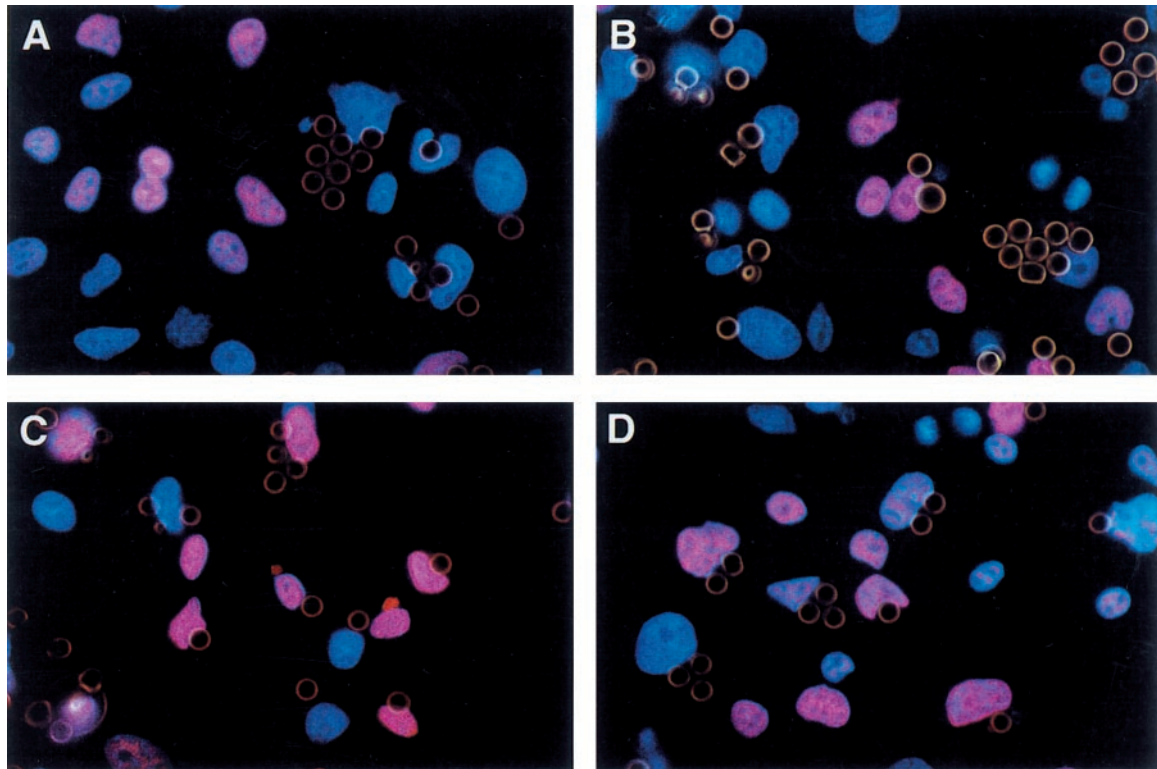
Figure 2 DAPI and BrdU staining of FL4 cells following incubation with cadherin-reactive and control beads. The cells were serum-starved for 72 h and then incubated in serum containing medium with beads (6 μm diameter) coupled to the following ligands: (**a**) recombinant NEC, (**b**) BE antibodies, (**c**) fibronectin and (**d**) ConA. The percentage of BrdU-positive cells was evaluated 24 h later by anti BrdU and DAPI labeling (see Materials and methods). Note that the BrdU-negative cells appear blue, while the BrdU-positive cells are pink. The beads are shown by phase contrast microscopy under low illumination (yellow)

Johnson *et al.*, 1994; Kato *et al.*, 1994). Within 24 – 48 h after serum stimulation with or without irrelevant beads the levels of p21 and p27 declined. This reduction in the levels of both cdk inhibitors could be effectively blocked by cadherin stimulation, using the NEC-coated beads (Figure 4b and c).

*Effect of cadherin-reactive beads on the cell cycle in exponentially growing cells*

To directly simulate adhesion-mediated effects on cell growth, we have incubated beads coupled to NEC, fibronectin or ConA with exponentially growing cells and studied their effect on the cell cycle using BrdU-DAPI quantitative double fluorescence microscopy (Figure 5). This approach enabled us to distinguish between G1, S and G2/M nuclei in the bead-associated cell population *in situ* (right column in Figure 5). These data indicated that the NEC-coated beads significantly reduce the percentage of cells in S-phase and increase the percentage of cells in G1, compared to control beads (Figure 6a). Immunoblotting analysis revealed a 2 – 3-fold increase in the total levels of p27, without a significant change in the levels of p21 (Figure 6b).

Discussion

The results presented above strongly suggest that adhesion-mediated signals, triggered by the clustering and/or immobilization of N-cadherin, suppress cell growth by arresting the cell cycle at the G1 phase. We

propose, on the basis of these results, that cadherin-mediated signaling is involved in contact-inhibition cell growth. While involvement of additional factors cannot be excluded, there is a remarkable similarity between the effect of cadherin-reactive beads and 'classical' contact inhibition in dense cultures: Contact inhibited cells tend to accumulate at the G1 phase of the cell cycle (Polyak *et al.*, 1994a) and the relative levels of hypophosphorylated pRb increase (Dietrich *et al.*, 1997), accompanied by accumulation of p27 (Dietrich *et al.*, 1997; Polyak *et al.*, 1994a) whose overexpression causes cell cycle arrest in G1 (Coats *et al.*, 1996). As outlined above, all these features of contact-inhibited cells are also observed in the cadherin-arrested cells.

While the growth inhibition by cadherin stimulation appears to induce an increase in p27 levels, the direct mechanism responsible for this increase is not yet clear. It was shown that in contact-inhibited cells, as well as in cells arrested in G1 by other mechanisms, the levels of p27 mRNA remain constant, suggesting that the observed increase in p27 protein levels is controlled by post-transcriptional mechanisms (Hengst and Reed, 1996). This is in line with the finding that the half-life of p27 is much longer in contact-inhibited cells compared to exponentially growing cells (Kato *et al.*, 1997) and that quiescent cells exhibit a lower level of p27 ubiquitinating activity compared to proliferating cells, which could account for the observed longer half-life of the molecule (Pagano *et al.*, 1995). In addition, the increase in the steady state levels of p27 can be attributed to translational upregulation of p27 synthesis (Hengst and Reed, 1996) or an increase in the
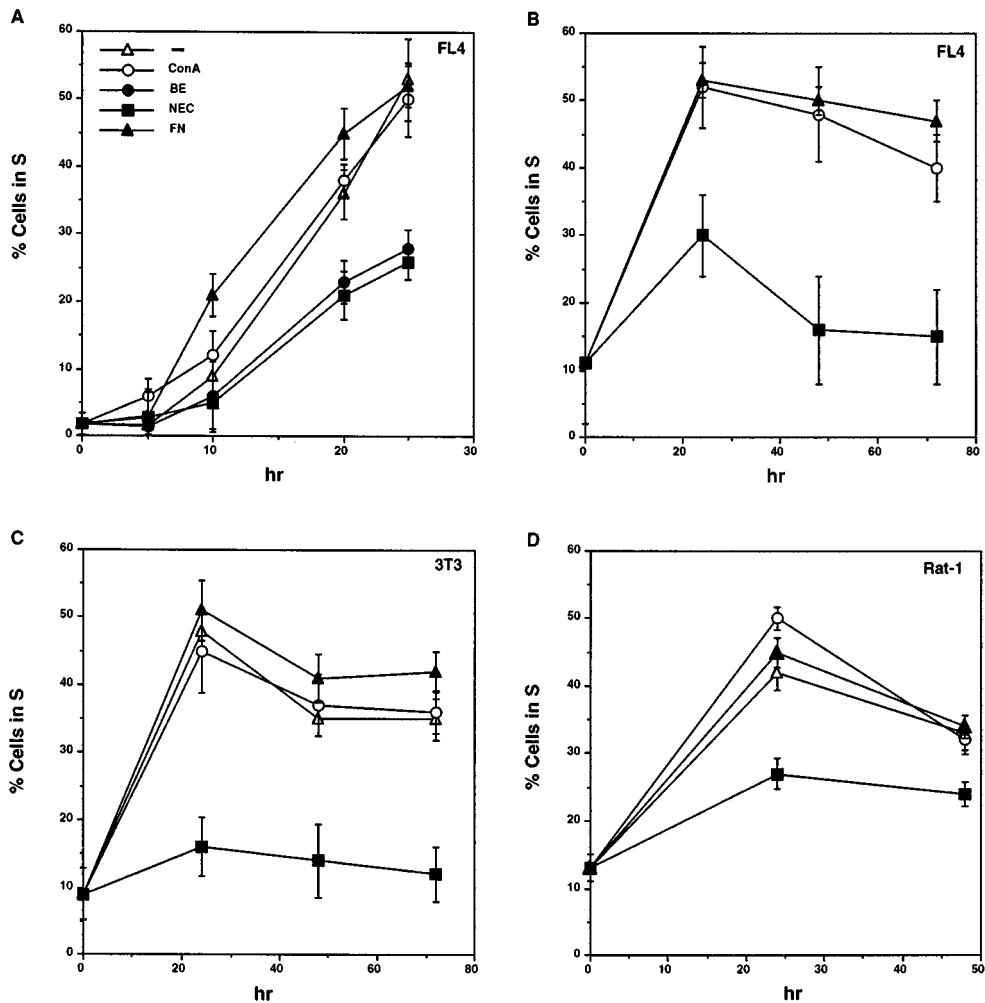
Figure 3 Effect of cadherin stimulation on the entry of serum-starved cells into S-phase following addition of serum. (a) N-cadherin expresssing CHO cells (FL4) were serum starved for 72 h after which 10% serum-containing medium was added for 24 h together with the cadherin-reactive beads (coated with NEC or BE) or beads coupled to FN or ConA. At each time point following serum stimulation (0 – 24 h) the percentage of BrdU-positive cells ('% cells in S') was evaluated by anti BrdU and DAPI double fluorescence labeling. (b – d) Effect of treatment with cadherin reactive beads and control beads on different cell lines including: FL4 (b), Swiss-3T3 (c) and Rat-1 (d). Cells were starved with medium containing low levels (0.1%) of serum for 48 h and then stimulated with 10% serum containing medium together with the beads (NEC, FN, ConA) and the percentage of BrdU-positive cells ('% cells in S') up to 72 h was evaluated as in **a**

amount of p27 polyribosome-bound-mRNA (Millard *et al.*, 1997). It is still unclear which of these possible mechanisms is directly affected by the cadherin-mediated signaling. Another member of the CIP/KIP family of cdk inhibitors, namely p21, was not elevated following incubation of growing (non starved) cells with cadherin-reactive beads, suggesting that it is not intimately involved in the cadherin-mediated G1 arrest. This is in contrast with the results obtained with serum starved cells. In these cells, both p27 and p21 were elevated and the cadherin-reactive beads inhibited the decline in the levels of both following serum stimulation. This indicates that the cadherin mediated signals block entry into S-phase of the cell cycle via different mechanisms in cycling and in serum-starved cells.

The approach employed here for cadherin simulation was primarily based on the use of cadherin-reactive beads to matrix-attached cells. This approach has some significant advantages over comparison of growth properties of cells expressing different levels of cadherin (as in Figure 1 here and Caveda *et al.*, 1996) since cell-cell contact mediated by specific cadherin molecules may promote additional molecular interactions involving additional membranal or secreted molecules. The application of cadherin-reactive beads to matrix-attached cells, as done here, rather than seeding cells on cadherin coated plates (Caveda *et al.*, 1996) has an additional advantage in that the observed effects can be directly attributed to the cadherin signaling, and not to perturbation of cell-matrix contacts and suppression of integrin signaling.

The notion that cadherin-mediated interactions can induce diverse long-range transmembrane signals was recently proposed by us, using a similar experimental approach (Levenberg *et al.*, 1998a). We showed that addition of N-cadherin-beads to CHO cells expressing modest levels of N-cadherin strongly stimulates tyrosine phosphorylation and assembly of adherens-junctions, and that this 'autoregulation' can be inhibited by tyrosine kianse-specific inhibitors (Levenberg *et al.*, 1998a). We are currently exploring the

question whether the two processes, namely the promotion of cell-cell adhesion and the growth suppression, are independent or interrelated, and search for specific tyrosine phosphorylation events which might be involved. It is noteworthy that

Figure 4 The effect of cadherin-reactive beads on pRb phosphorylation and the levels of p21 and p27 following starvation (STARV) and serum-stimulation. Equal amounts of Swiss-3T3 total cell protein were analysed 48 h after serum stimulation in the presence of the beads (NEC, BSA or ConA) or without beads (−) by SDS–PAGE followed by immunoblotting with pRb antibodies (**a**), p21 antibodies (**b**) and p27 antibodies (**c**). The ratio between hyposphorylated (Rb^{bp}) and phosphorylated (Rb^P) forms of pRb as well as the relative intensity of p21 and p27 in each sample were calculated based on three independent experiments and compared to those of starved cells

elevated expression of N-cadherin may also suppress cell locomotion and that its perturbation promotes cell motility (Huttenlocher et al., 1998; Levenberg et al., 1998b).

Another possible mechanism for the cadherin-mediated effect on cell growth may involve a modulation of the stability, availability or subcellular distribution of the cadherin-associated and signaling protein β-catenin (Huber et al., 1996; Miller and Moon, 1996; Peifer, 1997; van de Wetering et al., 1997). This possibility is supported by our recent studies showing that expression of cadherin and cadherin derivatives may alter the level and localization of β-catenin and consequently may affect its nuclear localization and signaling activity (Fagotto et al., 1996; Sanson et al., 1996) (Sadot E, Simcha I, Shutman M, Ben-Ze'ev A and Geiger B in preparation). It is an intriguing possibility that the recruitment or modulation of signaling molecules associated with adherens junctions, might be involved in signaling events such as the inhibition of cell growth and cell cycle progression as reported here.

Materials and methods

Cells

Chinese hamster ovary (CHO) cells, Rat-1 cells and Swiss-3T3 cells were obtained from the American Type Culture Collection (MD, USA). CHO cells were transfected with cDNA encoding chicken N-cadherin (kindly provided by M Takeichi, Kyoto University), subcloned into the pECE eukaryotic expression vector as described before (Levenberg et al., 1998a). Of the various stable clones generated, we have used for the beads assay the CHO-derived FL4 line which express relatively high levels of N-cadherin. The cells were maintained in Dulbecco's Modified Eagle Medium (DMEM) containing 10% fetal calf serum (Bio-Labs, Israel). Cells were cultured at 37°C in a humidified incubator under an atmosphere of 7% CO_2 and 95% air.
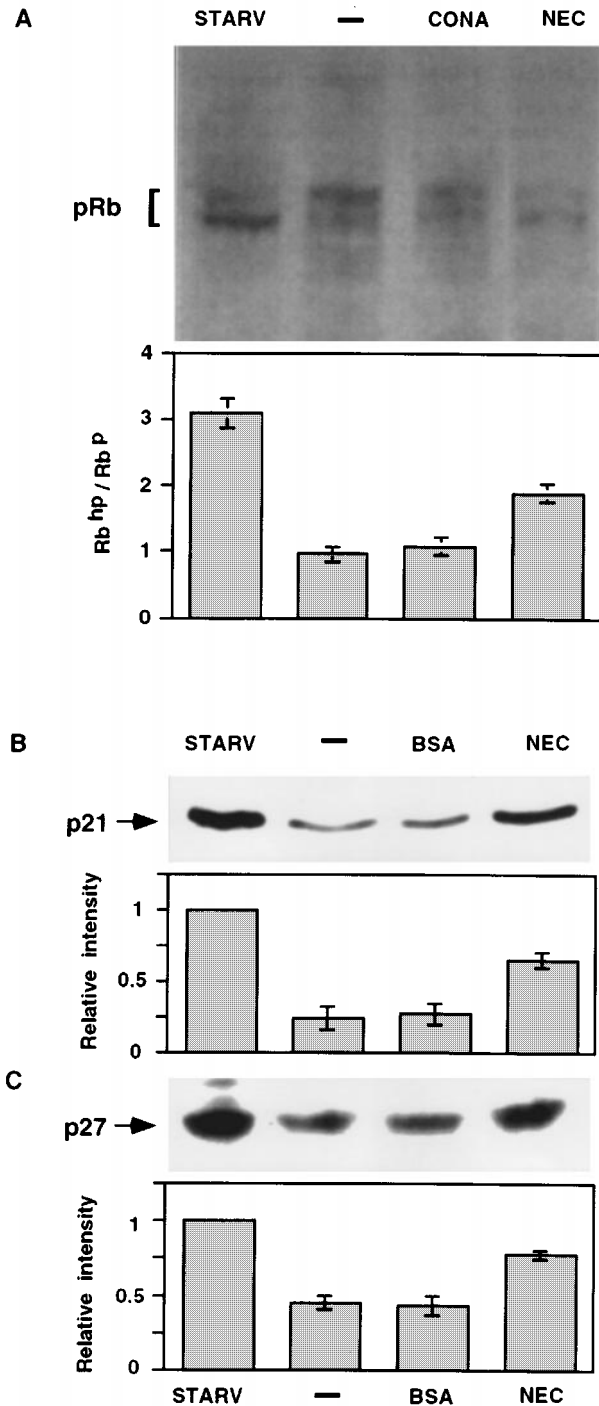
Cell growth and cell cycle analysis

To determined cell growth the cells were plated at about 20% confluence and the number of viable cells was counted in tetraplicates every day. In the inhibitory assay, the antibodies were added to the cells 24 h after seeding and the number of viable cells was determined in tetraplicates every day. Medium was changed every day and aliquots of antibodies (10 μl) added to 0.5 ml medium every 5 h. The antibodies that were used: N-cadherin-specific inhibitory antibodies (FA5) (Volk and Geiger, 1986) and control anti IL-2Rα antibodies (7G7).

When the distribution of cells in the different phases of cell cycle was determined by fluorescence-activated cell sorter analysis (FACS), subconfluent cultures were permeabilized with 0.1% Triton X-100, stained with propidum iodide and analysed using a FACScan cell sorter (Becton-Dickinson, Mountain View, CA, USA), and by applying the CellFitt program to determine the percentage of cells in the various stages of the cell cycle.

Production and purification of N-cadherin ectodomain (NEC)

To cluster N-cadherin, we have used a bacterially-expressed polypeptide corresponding to nearly the entire ectodomain of chicken N-cadherin (NEC). As previously described (Levenberg et al., 1998a), the cDNA encoding the ectodomain of chicken N-cadherin (from GAC 166 to

GAC 1720) was generated by the polymerase chain reaction (PCR) using full length chicken N-cadherin cDNA as a template, and inserted into the pET3d vector. To produce the cadherin ectodomain, competent BL21 cells were transformed with the pET3d construct, and the expression of the NEC was induced with IPTG using the T7 polymerase inducible pET system. The inclusion bodies were isolated and the protein extracted using GuHCl followed by renaturation in DTE/glutathione solution. The typical yield of NEC obtained from 500 ml of bacterial cultures was 10–20 mg.

Conjugation of proteins to synthetic beads

Polybead amino microspheres, mean diameter 6 μm (Polysciences Inc., Warrington, PA, USA) were washed with PBS at pH 7.4, incubated with 8% glutaraldehyde for 16 h with gentle mixing, followed by 5 h incubation with 500 μg/ml NEC, BE, FN or ConA (per 10^8 beads). The beads were then blocked by incubation with 0.5 M ethanolamine in PBS for 30 min followed by 30 min incubation with 10 mg/ml BSA and stored in PBS containing 10 mg/ml BSA, 0.1% NaN_3 and 5% glycerol.

Western blot analysis

Aliquots of cell extracts containing equal amounts of protein were resolved by 7.5% or 10% SDS–PAGE and electroblotted onto nitrocellulose filters. Blots were incubated with the primary antibodies followed by secondary antibodies conjugated to horseradish peroxidase using the ECL technique (Amersham, Little Shalfont,
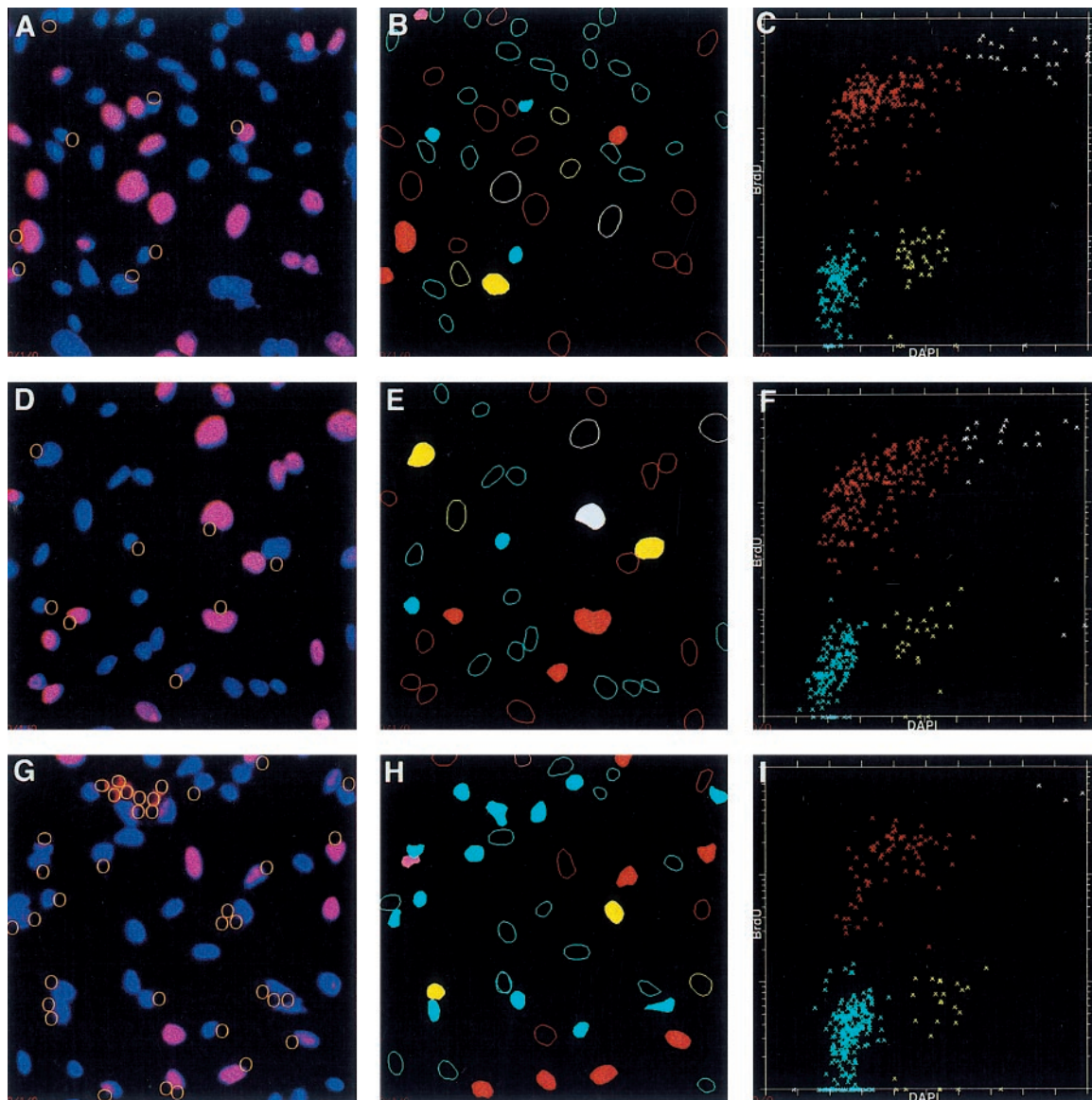
Figure 5 Effect of cadherin-reactive beads on the entry of FL4 cells into S-phase as determined by digital microscopy. Beads coated with ConA (**a**–**c**), FN (**d**–**f**) or NEC (**g**–**i**) were added to exponentially growing FL4 cells. Cell cycle distribution was determined microscopically using simultaneous quantitation of DAPI (as an indicator of DNA content) and incorporation of BrdU (as a marker for cells in S-phase). Images of DAPI-stained nuclei (blue), BrdU positive nuclei (pink) and the synthetic beads (marked yellow), are superimposed in **a**, **d** and **g**. The same fields are shown in **b**, **e** and **h**, where the outlined nuclei of cells which are associated with beads are filled and nuclei of cells which are not in direct contact with the beads are empty. The data obtained from 100 different images for each treatment, are shown in the dot-plots of BrdU fluorescent intensity (Y axis) *versus* DAPI fluorescent intensity (X axis) in **c**, **f** and **i**. The populations of G1, S and G2 nuclei are shown in light blue, red and yellow, respectively, in both the middle and the right columns. Cells with more than 4 n DNA, or small clusters consisting of two or more cells, are marked in white. These cells were not taken into account in the calculation

A

B
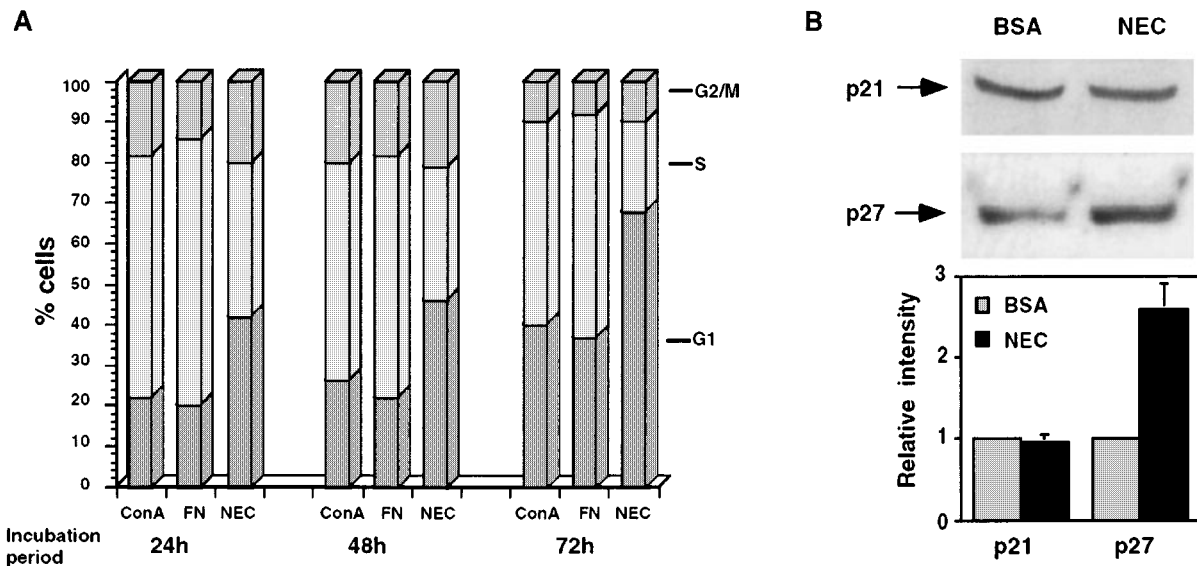
Figure 6 Cell cycle distribution and expression of p21 and p27 following cadherin stimulation as determined by digital fluorescence microscopy. (**a**) Beads (ConA, FN, NEC) were added to subconfluent monolayers of FL4 cells, for 24, 48 or 72 h. The cell cycle distribution was determined microscopically using simultaneous quantitation of DAPI and BrdU, and the percentage of cells in G1, S and G2 phases calculated according to the dot plots based on the digital fluorescent microscopic analysis (as in Figure 5 above). Standard deviations of the percentage of cells at S-phase were in the range of 1–7%. (**b**) The effect of cadherin-reactive beads on the levels of p21 and p27. Beads (BSA, NEC) were added to subconfluent monolayers of Swiss-3T3 cells for 24 h. Cells were then extracted and equal amounts of total cell protein were subjected to SDS–PAGE and immunoblotted with p21 and p27 antibodies. The relative intensity of the p21 and p27 bands in the cadherin-stimulated cells (NEC) was compared to that of control (BSA) cells in three independent experiments

UK). The antibodies used in this study included: Pan-cadherin antibody (CH19, Sigma Chemical Co., St Louis, MO, USA) pRb antibody (anti-human pRb, PharMingen, San Diego, CA, USA), p21 antibody (kindy provided by Dr C Schneider, University of Trieste, Italy) and p27 antibody (C-19, Santa Cruz Biotechnology, Inc., CA, USA).

BrdU labeling

Cells were incubated with BrdU for 30 min, fixed and permeabilized in 0.5% Triton X-100 and 3% paraformaldehyde in PBS for 3 min and post-fixed for 20 min with 3% paraformaldehyde. Following fixation, cells were treated with 2N HCl, 0.5% Triton for an additional 20 min, washed in PBS, and BrdU incorporation was visualized by indirect immunofluorescence staining with anti-BrdU antibodies (Becton-Dickinson, San Jose, CA, USA) and rhodamine-labeled goat anti-mouse antibodies (Jackson ImmunoResearch Laboratories, West Grove, PA, USA). Cells were co-stained with 5 μg/ml 4′,6-diamidino-2-phenylinodole (DAPI) to visualize nuclei.

Fluorescence microscopy and digital imaging

Images were acquired with a Zeiss Axioskop equipped with a cooled scientific grade CDD camera (CC/CE 200, Photometrics, Tucson, AZ, USA). The computerized microscope system (Kam *et al.*, 1993) and Prism software (Chen *et al.*, 1996) (Applied Precision Inc., Issaquah, WA, USA) included fast computer-controlled step-motors driving the excitation and emission filter wheels (Compu-motor, Petaluma, CA, USA). The filters are band-pass interference filters 'DF' type (excitation: 355 (band width = 40 nm) and 580 (20); emission: 425 (30) and 625 (30) for DAPI, and rhodamine respectively, and a

matching quadruple-wavelength dichroic mirror (Omega Co., Brattleboro, VT, USA), allowing to automatically acquire and process digital images of multiple-labeled samples. Images were online-corrected for inhomogeneous field illumination.

For fluorescence intensity measurements, the areas corresponding to nuclei are outlined in the DAPI images by polygons. Each polygon can be drawn automatically (based on segmentation algorithms), semi-automatically (by search for the decrease in intensity along radial lines emerging from a cursor-marked point inside each nucleus), or manually. Pixel values inside the polygon are added, and pixel values in the surrounding area are averaged to determine the local background for each nucleus. This process is repeated with the same polygon for all 'color components' of the image, in this case for the DAPI and BrdU images. This analysis produces a data file, listing, for each nucleus, its coordinates, integrated fluorescence intensities for DAPI and BrdU (as well as other morphological parameters which are irrelevant for this work). These data are analysed by a dot plot in which each nucleus is presented as a point in the corresponding DAPI and BrdU coordinates. The procedure is similar to standard flow cytometry, enabling the clear distinction of populations of S-phase cells (positive BrdU staining), G1-phase cells (low DAPI) and G2 phase cells (high DAPI).

References

Becker KF, Atkinson MJ, Reich U, Becker I, Nekarda H, Siewert JR and Hofler H. (1994). *Cancer Res.*, **54**, 3845 – 3852.

Caveda L, Martin-Padura I, Navarro P, Breviario F, Corada M, Gulino D, Lampugnani MG and Dejana E. (1996). *J. Clin. Invest.*, **98**, 886 – 893.

Chen H, Hughes DD, Chain TA, Sedat JW and Agard DA. (1996). *J. Struct. Biol.*, **116**, 56 – 60.

Coats S, Flanagan M, Nourse J and Roberts J. (1996). *Science*, **272**, 877 – 880.

Deleu L, Fuks F, Spitkovsky D, Horlein R, Faisst S and Rommelaere J. (1998). *Mol. Cell. Biol.*, **18**, 409 – 419.

Dietrich C, Wallenfang K, Oesch F and Wieser R. (1997). *Oncogene*, **15**, 2743 – 2747.

Fagotto F, Funayama N, Gluck U and Gumbiner BM. (1996). *J. Cell. Biol.*, **132**, 1105 – 1114.

Hengst L and Reed S. (1996). *Science*, **271**, 1861 – 1864.

Hollery RW. (1975). *Nature*, **258**, 487 – 490.

Huber O, Bierkamp C and Kemler R. (1996). *Curr. Opin. Cell Biol.*, **8**, 685 – 691.

Huttenlocher A, Lakonishok M, Kinder M, Wu S, Truong T, Knudson KA and Horwitz AF. (1998). *JCB*, **141**, 515 – 526.

Johnson M, Dimitrov D, Vojta PJ, Barrett JC, Noda A, Pereira-Smith OM and Smith JR. (1994). *Mol. Carcinog.*, **11**, 59 – 64.

Kam Z, Jones MO, Chen H, Agard DA and Sedat JW. (1993). *Bioimaging*, **1**, 71 – 81.

Kandikonda S, Oda D, Niederman R and Sorkin B. (1996). *Cell Adhes. Comm.*, **4**, 13 – 24.

Kato A, Takahashi H, Takahashi Y and Matsushime H. (1997). *J. Biol. Chem.*, **272**, 8065 – 8070.

Kato JY, Matsuka M, Polyak K, Massague J and Sherr C. (1994). *Cell*, **79**, 487 – 496.

Levenberg S, Katz BZ, Yamada KM and Geiger B. (1998a). *J. Cell. Sci.*, **111**, 347 – 357.

Levenberg S, Sadot E, Goichberg P and Geiger B. (1998b). *Cell Adhe. Commun.*, In press.

Millard S, Yani JS, Nguyen H, Pagano M, Kiyokawa H and Koff A. (1997). *J. Biol. Chem.*, **272**, 7039 – 7098.

Miller JR and Moon RT. (1996). *Genes Dev.*, **10**, 2527 – 2593.

Pagano M, Tam SW, Theodoras AM, Beer-Romero P, Del Sal G, Chau V, Yew PR, Dretta GF and Rolf M. (1995). *Science*, **269**, 682 – 685.

Peifer M. (1997). *Science*, **275**, 1752 – 1753.

Polyak K, Kato J, Solomon MJ, Sherr CJ, Massague J, Roberts JM and Koff A. (1994a). *Genes & Develop.*, **8**, 9 – 22.

Polyak K, Lee MH, Erdjument-Bromage H, Koff A, Roberts JM, Tempst P and Massague J. (1994b). *Cell*, **78**, 59 – 66.

Sanson B, White P and Vincent JP. (1996). *Nature*, **383**, 627 – 630.

Tsukita S, Itoh M, Nagafuchi A, Yonemura S and Tsukita S. (1993). *J. Cell. Biol.*, **123**, 1049 – 1053.

van de Wetering M, Cavallo R, Dooijes D, van Beest M, van Es J, Loureiro J, Ypma A, Hursh D, Jones T and Bejsovec A. (1997). *Cell*, **88**, 789 – 799.

Volk T and Geiger B. (1986). *J. Cell Biol.*, **103**, 1451 – 1464.

Weiser RJ, Heck R and Oesch F. (1985). *Exp. Cell Res.*, **158**, 493 – 499.

Weiser RJ and Oesch F. (1986). *J. Cell Biol.*, **103**, 361 – 367.